

Mapping the evolution of Bi/Ge(111) empty states: From the wetting layer to pseudo-cubic islands ^{EP}

Cite as: J. Appl. Phys. **129**, 155310 (2021); <https://doi.org/10.1063/5.0048275>

Submitted: 21 February 2021 . Accepted: 29 March 2021 . Published Online: 21 April 2021

^{id} F. Goto, ^{id} A. Calloni, ^{id} G. Albani, ^{id} A. Picone, ^{id} A. Brambilla, ^{id} C. Zucchetti, ^{id} F. Bottegoni, ^{id} M. Finazzi, L. Duò, F. Ciccacci, and ^{id} G. Bussetti

COLLECTIONS

^{EP} This paper was selected as an Editor's Pick



View Online



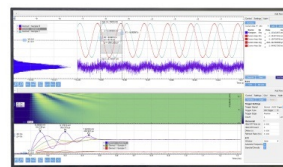
Export Citation



CrossMark

Challenge us.

What are your needs for
periodic signal detection?



Zurich
Instruments

Mapping the evolution of Bi/Ge(111) empty states: From the wetting layer to pseudo-cubic islands



Cite as: J. Appl. Phys. 129, 155310 (2021); doi: 10.1063/5.0048275

Submitted: 21 February 2021 · Accepted: 29 March 2021 ·

Published Online: 21 April 2021



F. Goto, A. Calloni, G. Albani, A. Picone, A. Brambilla, C. Zucchetti, F. Bottegoni, M. Finazzi, L. Duò, F. Ciccacci, and G. Bussetti

AFFILIATIONS

Dipartimento di Fisica, Politecnico di Milano, Piazza Leonardo da Vinci 32, 20133 Milano, Italy

^{a)}Author to whom correspondence should be addressed: alberto.calloni@polimi.it

ABSTRACT

Semiconductors interfaced with heavy elements possessing a strong atomic spin-orbit coupling are important building blocks for the development of new spintronic devices. Here, we present a microscopic and spin-resolved spectroscopic investigation of ultrathin Bi films grown onto a Ge(111) substrate. At monolayer coverage, a Bi wetting layer is formed, characterized by a semiconducting behavior and a $(\sqrt{3} \times \sqrt{3})R30^\circ$ superstructure. The wetting layer supports the subsequent growth of Bi islands with a pseudo-cubic structure similar to that of Bi(110), showing a well-defined orientation with respect to the substrate high-symmetry directions. We performed photoemission and spin-resolved inverse photoemission experiments at off-normal electron emission and incidence, respectively, along the substrate $\Gamma\bar{K}$ direction. Inverse photoemission, in particular, highlights the presence of a spin-polarized empty Bi state, not reported so far, due to the strong spin-orbit effects characteristic of the Bi surface and thin layers. Finally, scanning tunneling spectroscopy is employed to link the observed spectroscopic features to either the wetting layer or the Bi islands.

Published under an exclusive license by AIP Publishing. <https://doi.org/10.1063/5.0048275>

INTRODUCTION

Bismuth thin films are the focus of many research efforts since the advent of advanced growth and characterization techniques capable of investigating and controlling the peculiar morphology stemming from the Bi interaction with its substrate.^{1,2} On semiconductors, Bi is generally reported to grow according to the Stranski-Krastanov mode, i.e., by forming 3D structures with a structure resembling that of bulk Bi above a first wetting layer commensurate with the substrate lattice.^{3,4} At larger Bi thickness, islands coalescence can be promoted in order to flatten the surface morphology and achieve long range crystallographic order.^{3,5,6} The presence of an abrupt interface with the substrate with no intermixing,^{7,8} the possibility of realizing a variety of growth morphologies, and the particular electrical and transport properties (see, e.g., Ref. 9 for a review) make Bi films an ideal playground to investigate many different physical phenomena. Among others, we recall quantum and finite size effects,¹⁰⁻¹² semimetal to semiconductor (SMSC) transitions,¹³ and thermoelectric^{14,15} and magnetoresistive^{16,17} effects.

Bi surfaces and thin layers are also regarded as prototypical systems for the study of the peculiar electronic structure stemming

from a strong spin-orbit coupling (SOC). Thanks to the high atomic number, bulk Bi states show a SOC splitting in the electron-volt range,¹⁸ which, however, does not lead to any spin-polarized bands due to the presence of lattice structure inversion symmetry. Conversely, electron localization at surfaces or interfaces can develop spin-split electronic states due to the breaking of such symmetry (the so-called Rashba effect).¹⁹ Noteworthy examples are the electronic states of the Bi/Ag(111) surface alloy²⁰ and the β -Bi/Si(111)- $\sqrt{3} \times \sqrt{3}$ surface.²¹ In addition, a complicated “spin texture” is found at the surfaces of either bulk Bi^{18,22,23} or Bi alloys.^{24,25} In semi-metallic Bi, spin-related effects involving electron transport are enhanced due to the limited contribution to the electrical conductivity coming from bulk electronic states, making these systems very attractive for applications in the field of spintronics.²⁶

Spin-resolved photoemission spectroscopy (SR-PES) is the technique of choice to map the electronic structure of Bi surfaces and thin films, being also sensitive to the peculiar spin texture stemming from the presence of SOC effects. Complementary to SR-PES are spin-resolved inverse photoemission spectroscopy (SR-IPES),²⁷ and scanning tunneling

spectroscopy (STS),²⁸ providing information also on empty electronic states. Both techniques have been synergistically employed in the past for the characterization of Bi growth on III-V semiconductors such as, for instance, GaAs^{29,30} and also found application in the study of a variety of homo- and hetero-structures showing SOC related effects.^{31–33}

In the present contribution, we focus on the morphological and electronic evolution of the Bi/Ge(111) system. For increasing Bi coverage, a wetting layer is first formed where the Bi atoms are arranged in a $(\sqrt{3} \times \sqrt{3})R30^\circ$ superstructure, characterized by the presence of spin-polarized Rashba electronic states at specific high-symmetry points of the Surface Brillouin Zone (SBZ).^{34,35} At larger Bi coverages, pseudo-cubic Bi islands are formed, showing a metastable pseudo-square surface lattice. Bi islands eventually merge into a continuous film with the same hexagonal symmetry of the substrate.^{36,37} We have previously investigated the spin texture of this particular system with SR-PES^{35,37} and SR-IPES (the latter exploited only for the wetting layer).³⁵ In this work, we investigate the empty states of the metastable Bi layers for which no information can be found in the literature.

EXPERIMENTAL

Bi was grown on a Sb-doped Ge(111) substrate (resistivity $\rho = 0.18 \Omega \text{ cm}$) cleaned by cycles of sputtering with 1 kV Ar^+ ions followed by thermal annealing at 900 °C. The quality of the substrate was addressed by photoemission, confirming the absence of any detectable amount of surface contaminants, and low-energy electron diffraction (LEED), showing the characteristic $c(2 \times 8)$ pattern typical of the vacuum-cleaned Ge(111) surface.³⁸ Bi was thermally evaporated at a rate of about 1 \AA min^{-1} from a BN crucible. The $(\sqrt{3} \times \sqrt{3})R30^\circ$ Bi superstructure was produced by annealing at 450 °C a film of a nominal thickness slightly in excess of 2.6 Å, evaluated by means of a quartz microbalance, corresponding to the amount of atoms required to completely cover (assuming a perfect epitaxy) the Ge(111) surface.^{36,39} Subsequent layers were grown keeping the sample at room temperature (RT) without any further post-growth treatment. Photoemission spectroscopy data were collected on a system equipped with a 150 mm hemispherical analyzer and an unpolarized HeI source. *In situ* SR-IPES spectra were acquired in the isochromatic mode (by detecting 9.6 eV photons)

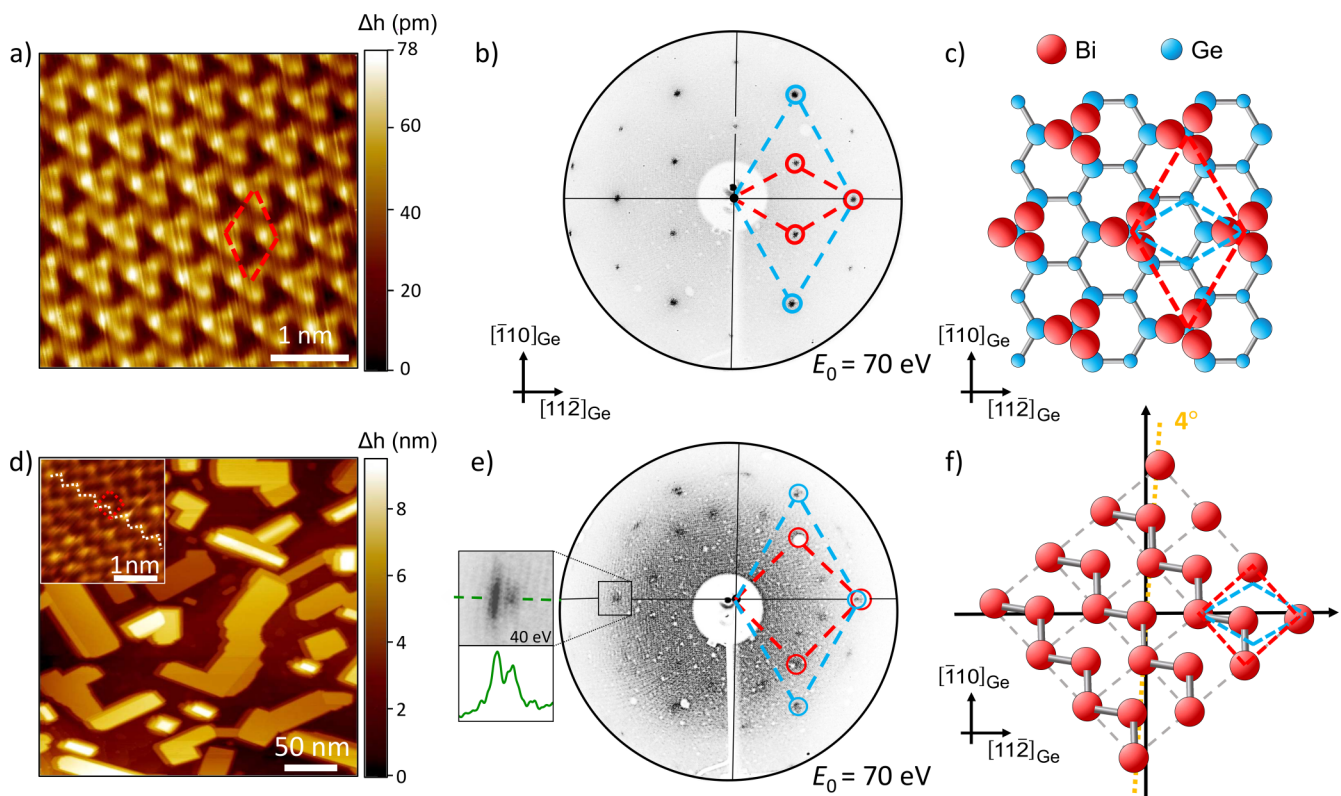


FIG. 1. (a) STM image ($I_{\text{tunnel}} = 5 \text{ nA}$; $V_{\text{bias}} = 0.6 \text{ V}$), (b) LEED pattern, and (c) schematic top view of the $(\sqrt{3} \times \sqrt{3})R30^\circ$ Bi/Ge(111) system. Blue (red) lines in (b) and (c) mark the Ge (Bi) unit cells in the reciprocal and real space, respectively. (d) STM image ($I_{\text{tunnel}} = 1 \text{ nA}$; $V_{\text{bias}} = 1 \text{ V}$) acquired at a nominal Bi thickness of about 20 Å. In the top-left inset: atomic resolution on top of a Bi island ($I_{\text{tunnel}} = 5 \text{ nA}$ and $V_{\text{bias}} = 0.1 \text{ V}$). (e) LEED pattern acquired on the thick Bi film. A close up of a selected diffraction spot, acquired at a slightly lower beam energy, is printed together with its intensity profile along the $[112]_{\text{Ge}}$ direction. (f) Schematic of a pseudo-cubic (PC) domain with the diagonal rotated by 4° with respect to the $[110]_{\text{Ge}}$ axis.

with a home-built apparatus characterized by a Full Width at Half Maximum (FWHM) energy and angular resolution of 0.7 eV and 3° , respectively.⁴⁰ The source of spin-polarized electrons was a GaAs (100) photocathode excited with circularly polarized light.⁴¹ All photoemission measurements were acquired with the sample kept at 100 K. The STM and STS measurements have been collected at RT by using an Omicron variable temperature microscope with home-made electrochemically etched W tips. STM topographic images have been acquired in constant-current mode. STS spectra for the characterization of the sample density of states have been obtained by using a lock-in amplifier by modulating the sample bias with a sinusoidal signal with an amplitude of 40 mV.

RESULTS AND DISCUSSION

The results of our structural characterization of the system under study are shown in Fig. 1 for the $(\sqrt{3} \times \sqrt{3})R30^\circ$ Bi surface [panels (a)–(c)] and a thick (about 20 Å) Bi film [panels (d) and (e)].

The STM image of panel (a) shows that Bi atoms, ideally filling all the adsorption sites of the (111) surface at monolayer coverage, are organized in trimers forming a larger hexagonal lattice: it is the so-called T4 or “milkstool” arrangement.⁴² Panel (b) shows the LEED pattern of the reconstructed Bi surface: the unit cell of the Bi layer reconstruction (red parallelogram) is smaller but still commensurate with the one of the Ge(111) substrate (blue parallelogram). In real space [panel (c)] the arrangement of Bi trimers can be obtained by rescaling ($a_{\sqrt{3}} = \sqrt{3} \cdot a_{\text{Ge}(111)}$), and rotating by 30° the Ge lattice unit cell, hence the $(\sqrt{3} \times \sqrt{3})R30^\circ$ label.

Subsequent Bi layers were grown step-by-step on top of the $(\sqrt{3} \times \sqrt{3})R30^\circ$ wetting layer. The STM image of Fig. 1(d) shows that Bi islands are formed, contributing to the LEED diffraction pattern of panel (e). The LEED result is linked to the establishment of a metastable pseudo-cubic (PC) phase,³ where Bi atoms form a pseudo-square lattice at the surface, similar to that of the (110) face of bulk bismuth (note that Miller indices for bulk Bi are given

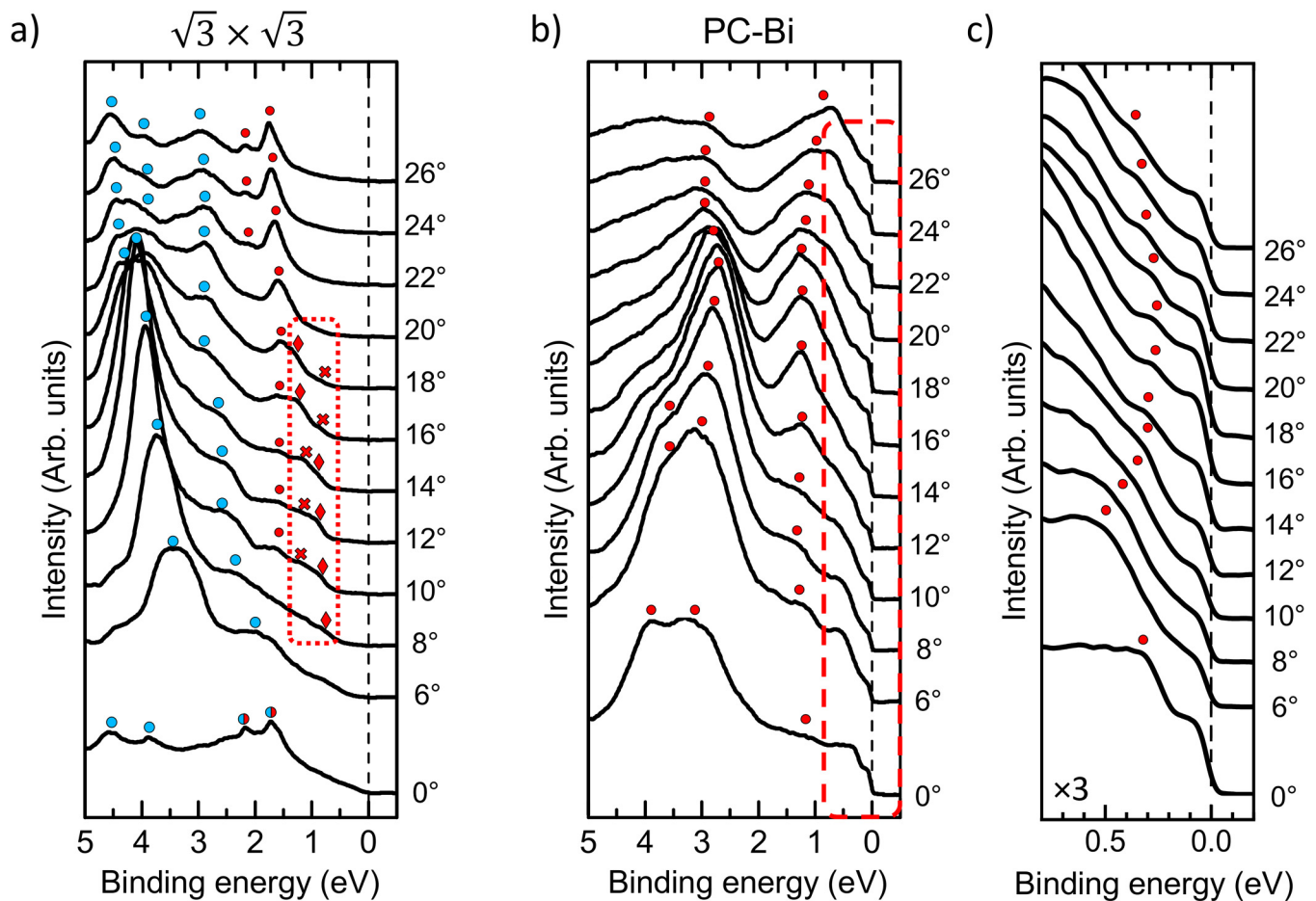


FIG. 2. (a) Angle-resolved PES spectra for the $\sqrt{3} \times \sqrt{3}$ reconstruction. The region featuring Bi states with a Rashba-like dispersion (see the text for more details) is enclosed by red dotted lines. (b) PC-Bi at a nominal thickness of about 20 Å. On the right (c), the red box in (b) is expanded in order to better resolve the Fermi region. Blue (red) symbols, associated to Ge (Bi) spectral features, are added as a guide to the eye.

according to the rhombohedral lattice notation³⁶). Since there is one mirror plane in the PC unit cell, two mirror domains are formed along each equivalent $\langle 11\bar{2} \rangle_{\text{Ge}}$ direction, for a total of six equivalent PC domains [one of those is shown with red lines in panel (e)]. The PC lattice is not fully commensurate with the substrate, as shown in the magnified detail of Fig. 1(e), where the selected diffraction spot appears to be split along the $[11\bar{2}]_{\text{Ge}}$ direction with $k_{\text{Ge}} = (0.96 \pm 0.04)k_{\text{Bi}}$.

Starting from the LEED image, it is possible to picture a real space schematic of a pseudo-square Bi domain [Fig. 1(f)]. Following Ref. 43, we detect a rotation by $4 \pm 1^\circ$ of the pseudo-square lattice with respect to one of the three equivalent $\langle 11\bar{2} \rangle_{\text{Ge}}$ directions. The tilting angle is determined on LEED images acquired at a lower beam energy (data not shown). The observed splitting of the diffraction

spots accounts for the relaxation of the PC-Bi surface toward the ideal bulk-like Bi(110) lattice, considering that a perfect coincidence of the Ge(111) and PC-Bi lattices along the $[11\bar{2}]_{\text{Ge}}$ direction would instead result in a large strain of about 5.5% along the PC unit cell diagonal $[(d_{\text{PC}}^{\text{coinc}} - d_{\text{PC}}^{\text{bulk}})/d_{\text{PC}}^{\text{bulk}}]$, with $d_{\text{PC}}^{\text{bulk}} = 6.57 \text{ \AA}$ and $d_{\text{PC}}^{\text{coinc}} = a_{\text{Ge}} \cdot \sqrt{3} = 6.93 \text{ \AA}$. According to Fig. 1(f), Bi atoms are displaced in a “zig-zag” fashion,^{36,44} consistent with the STM image shown in the inset of panel (d), where atomic resolution is achieved on top of one island.

Our photoemission characterization of the Bi/Ge(111) system is shown in Fig. 2. Angle-resolved spectra are acquired by rotating the sample around the $[11\bar{2}]_{\text{Ge}}$ direction, in order to probe the momentum dispersion along the $\Gamma\bar{K}$ direction of the Ge (111) SBZ. Panel (a) shows the angle-resolved spectra from the wetting layer. Bulk Ge states, marked in blue, disperse toward

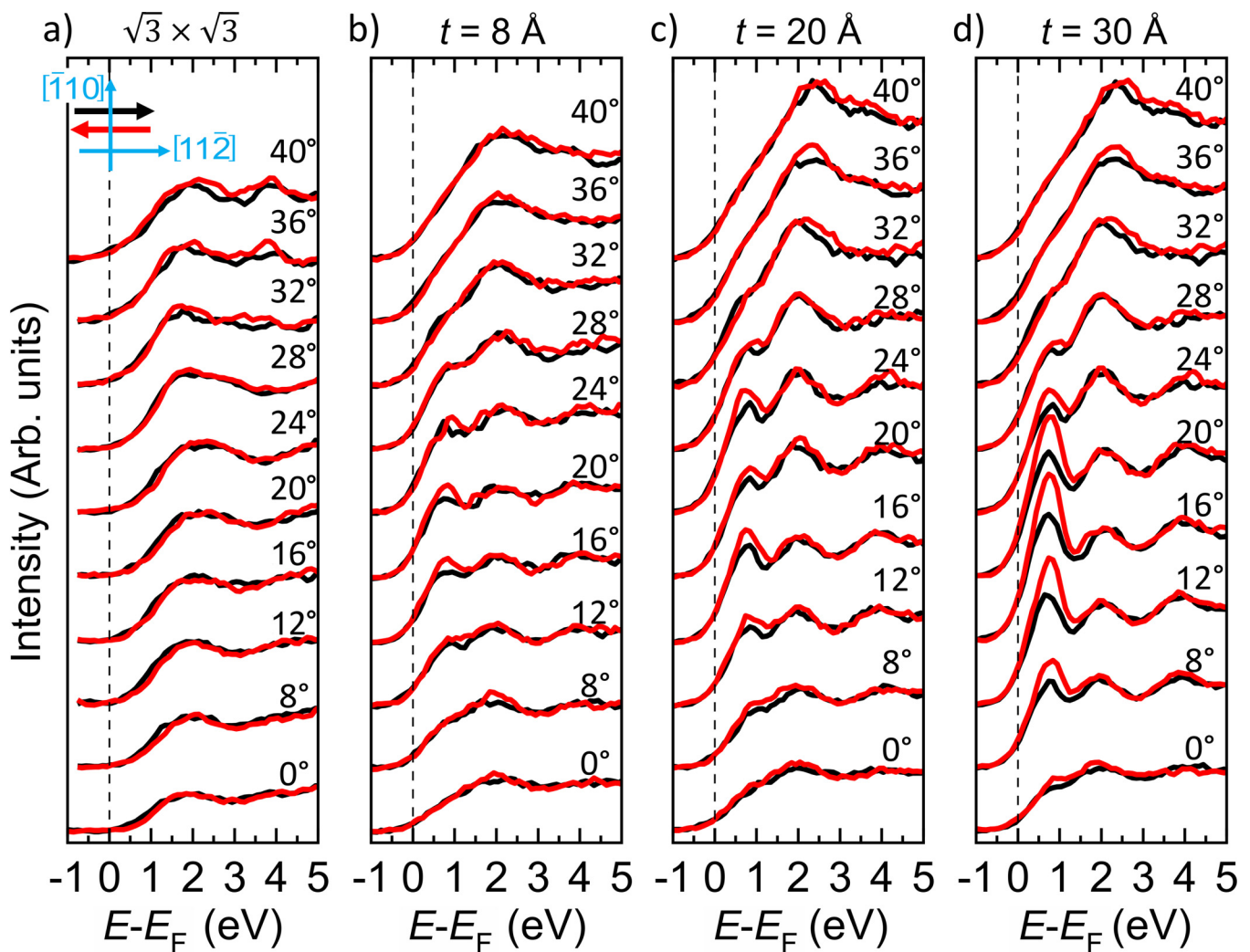


FIG. 3. (a)–(d) Spin- and angle-resolved IPES spectra for $(\sqrt{3} \times \sqrt{3})R30^\circ$ Bi and Bi layer with nominal thicknesses $t = 8 \text{ \AA}$, $t = 20 \text{ \AA}$, and $t = 30 \text{ \AA}$. Black (red) lines refer to spectra acquired with electrons spin-polarized parallel (antiparallel) to the $[11\bar{2}]_{\text{Ge}}$ direction.

higher binding energy (BE) with increasing emission angle. Bi surface bands related to the $(\sqrt{3} \times \sqrt{3})R30^\circ$ reconstruction are marked in red. Close to the $\bar{\Gamma}$ point, Bi bands are located in a region of not nil density of bulk Ge states and, therefore, have a resonant character.^{34,35} Around the \bar{M}' point ($\approx 16^\circ$) of the $(\sqrt{3} \times \sqrt{3})R30^\circ$ SBZ [red box in Fig. 2(a)], a Rashba-like dispersion of Bi states is instead observed, as we reported by means of spin- and angle-resolved photoemission spectroscopy in our previous work.³⁵

In the ultrathin limit of the wetting layer, the Bi/Ge(111) system is not metallic, as also confirmed by STS measurements (see below). Conversely, a metallic character characterizes the electronic structure of Bi in the metastable PC phase [Fig. 3(b)], as suggested by the presence of a clearly visible Fermi edge at all angles. Bi states are observed at ≈ 3 and 1 eV and show a small energy dispersion.

We attribute them mainly to bulk Bi emission by comparison with previous literature works on Bi thick films.^{45,46} The electronic states dispersion for the metastable PC phase is clearly different from the one characteristic of the two-dimensional Bi limit (i.e., the wetting layer). Some differences are also noted with the stable hexagonal phase observed in the case of thicker Bi films (see, e.g., Refs. 37 and 47) whose discussion falls, however, outside the scope of the present work. Other states characterized by a smaller photoemission intensity are found within approximately 0.5 eV from the Fermi level (E_F). A close up of the spectra in this energy region is reported in panel (c). According to the literature, we attribute the observed photoemission signal to surface states.^{37,47} As demonstrated by means of spin-resolved PES,³⁷ such surface states are spin polarized.

Empty states are studied by means of SR-IPES for increasing Bi thickness, as shown in Figs. 3(a)–3(d). As for the previous

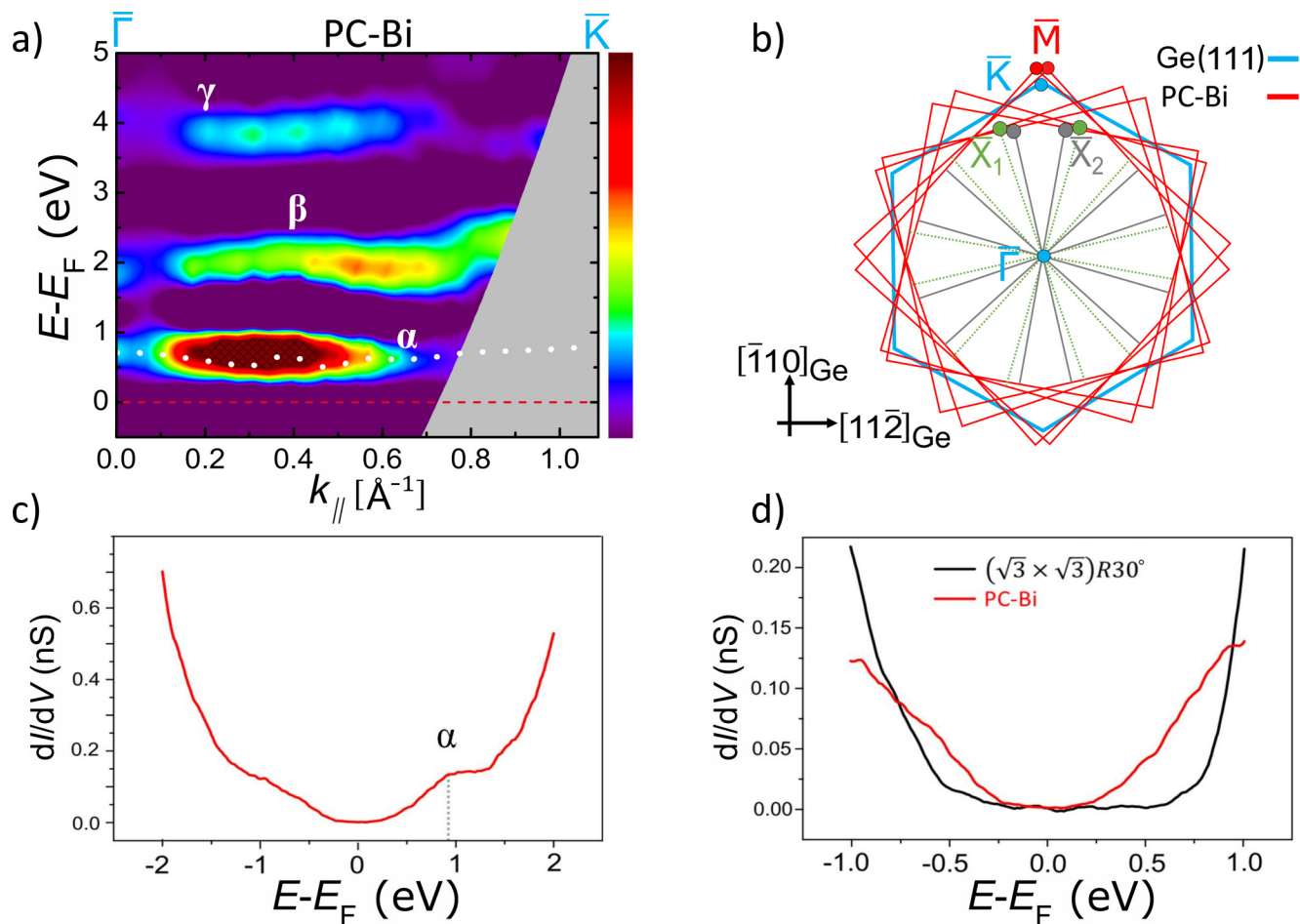


FIG. 4. (a) Spin-integrated IPES contour map as a function of the surface wave vector, $k_{||}$, along the $\bar{\Gamma}\bar{K}$ direction at a nominal thickness of $t = 30$ \AA . (b) Schematic of six PC SBZs (red) on top of the hexagonal substrate SBZ (light blue). (c) Representative STS spectrum of the electronic structure of PC-Bi islands. (d) Close up of the spectrum in (c) in a region close to E_F (red line), plotted together with the STS spectrum acquired on the $(\sqrt{3} \times \sqrt{3})R30^\circ$ Bi wetting layer (black line). Tunnel parameters in both cases are $I_{\text{tunnel}} = 400$ pA and $V_{\text{bias}} = 1.3$ V.

photoemission results, IPES spectra are acquired by scanning the electron momentum along the $\bar{\Gamma}\bar{K}$ direction of the substrate SBZ and with an electron spin polarization parallel to the $[11\bar{2}]_{\text{Ge}}$ direction. The spectra coming from the $(\sqrt{3} \times \sqrt{3})R30^\circ$ system [see panel (a)] are largely dominated by photoemission from the Ge (111) substrate. A faint Rashba-like spectral asymmetry is detected at about 2 eV in the momentum region corresponding to the \bar{M}' point of the $(\sqrt{3} \times \sqrt{3})R30^\circ$ SBZ (between 16° and 28° , see Ref. 37 for further information). At larger Bi coverages, a new photoemission feature develops between 8° and 24° , peaking at an energy of 0.8 eV. The intensity of such a feature increases for increasing Bi thickness. It is interesting to note an analogy between the present IPES results and a number of studies in the literature on the Bi/GaAs(110) system. Its structural evolution also bears some resemblance to the Bi/Ge(111) one: after the formation of a (1×1) wetting layer, islands develop with a metastable pseudo-square surface lattice compatible with the $(10\bar{1})$ surface of bulk Bi⁴. In the Bi/GaAs(110) system, the appearance of a peak close to E_F is reported for Bi thicknesses above the first (wetting) layer,^{30,48} i.e., concomitant to the development of a PC-Bi phase. At variance with previous IPES works and thanks to the spin resolution, however, our results highlight a strong spin polarization of such a feature, reaching a value of $(15 \pm 4)\%$ at a nominal thickness of 30 Å.

In order to describe the momentum dispersion of the Bi states observed on thick layers, the second derivative of the spectra of Fig. 3(d) is plotted as a spin-integrated contour map in Fig. 4(a). The white dashed line marks the lower limit of the surface-projected bulk band structure of Bi(110) along the PC-Bi $\bar{\Gamma}\bar{M}$ direction, taken from Ref. 49. As explained in the Experimental section, the sample surface is populated by 6 PC-Bi domains oriented in different directions. Each domain contributes to the measured electronic dispersion and is characterized by its own SBZ, as reported in panel (b) (red parallelograms), where the blue hexagon is related to the Ge(111) substrate SBZ. The IPES signal recorded along the Ge(111) $\bar{\Gamma}\bar{K}$ direction is, therefore, made up of different contributions coming from electronic states characteristic of the high symmetry $\bar{\Gamma}\bar{X}_{1,2}$ and $\bar{\Gamma}\bar{M}$ PC-Bi directions. Following photoemission studies on the same or similar systems featuring PC-Bi islands,^{37,47} we expect a dominant contribution to the measured spectra coming from the Bi $\bar{\Gamma}\bar{M}$ direction also for IPES. By inspecting the 2D map of Fig. 4(a), we recognize the presence of three states (α , β , γ). α is the spin-polarized state at an energy of 0.8 eV reported in Fig. 3(d), while β and γ are spin degenerate Bi states visible at all incidence angles and showing a slight upward energy dispersion towards the \bar{K} point of the Ge(111) SBZ.

A STS spectrum representative of PC-Bi islands is shown in Fig. 4(c). The position of feature α is highlighted with a vertical dotted line. As explained in Ref. 50, due to geometrical considerations related to the position of the STM probe (normal to the surface), STS spectra are much more sensitive to electronic states close to the $\bar{\Gamma}$ point of the SBZ with $k_{\parallel} \leq 0.1 \text{ \AA}^{-1}$. This explains the lower visibility of state α with respect to the results of Fig. 3(d). The intensity and energy dispersion of such a feature is nevertheless compatible with the IPES result obtained at normal electron incidence. In Fig. 4(d), we plot a close up of the STS spectra acquired in an energy region around E_F for the $(\sqrt{3} \times \sqrt{3})R30^\circ$ wetting layer (black line) together with the result related to PC-Bi

islands (red line). The different curvature of the two spectra is consistent with the different electrical behaviors of the two surfaces retrieved from our photoemission characterization: insulating that of the $(\sqrt{3} \times \sqrt{3})R30^\circ$ layer and semi-metallic the one of the PC-Bi islands. The momentum dispersion of feature α , overlapping with the lower limit of the surface-projected bulk band structure, is compatible with the expected behavior of Bi(110) surface states which, according to simulations, depart from E_F away from high-symmetry points of the PC-Bi SBZ.^{49,51} Considering also the extreme surface sensitivity of the STS technique, we predict for state α a large spectral contribution in the surface region, characteristic of surface resonances.

We now turn our attention to the large spin polarization observed in IPES spectra. Thanks to a proper choice of the experimental geometry, with the photoemission reaction plane (i.e., the plane identified by the momenta of the impinging electrons and the detected photons) orthogonal to the direction of the electron spin polarization, we are sensitive to (i) the intrinsic polarization of the investigated states and (ii) dichroic effects related to photoemission transition matrix elements.^{52,53} For what concerns point (i), the chosen spin polarization direction is indeed consistent with the momentum-locking condition characteristic of Rashba states. In all cases, given the centrosymmetric nature of bulk Bi, the observation of a spectral spin asymmetry relies on the presence of strong SOC effects involving the α state (final state of the inverse photoemission process), in turn related to details such as its spatial localization and orbital symmetry.^{54,55} In general, such an interplay of different contributions makes the interpretation of spin-resolved results in the presence of strong SOC effects particularly challenging but nevertheless worth of being investigated, given the rich physics involved and the technological importance of such systems (see, e.g., Refs. 56 and 57 and Refs. 55 and 58 for recent results obtained with SR-PES and SR-IPES, respectively). Our contribution therefore represents a first step toward a more complete understanding of the spin texture of Bi empty states in metastable films and at the Bi/semiconductor interface.

CONCLUSIONS

We investigated the electronic structure and morphology of ultrathin Bi layers grown onto a Ge(111) substrate with a $(\sqrt{3} \times \sqrt{3})R30^\circ$ Bi wetting layer interposed at the semiconductor interface. In agreement with previous studies, we report on the formation of Bi islands showing a well-defined orientation and a metastable pseudo-cubic structure, showing a pseudo-square surface. Clear signatures of the metastable phase are detected by means of photoemission and inverse photoemission spectroscopy. In particular, an intense feature with a clearly detectable spin polarization reaching its maximum intensity at slightly off-normal electron incidence characterizes the inverse photoemission signal from empty states. Such a feature, located slightly above the Fermi level, is observed also by scanning tunneling spectroscopy performed on top of the Bi islands. The detection of spin asymmetry in the photoemission spectra results from the strong spin-orbit coupling shaping the Bi band structure. For empty states, it appears confined in a specific energy and momentum region, an important finding

in view of improving the effectiveness of spin manipulation in metastable Bi films and Bi/Ge(111) hetero-structures.

ACKNOWLEDGMENTS

The authors would like to thank A. Camera for fruitful discussions.

DATA AVAILABILITY

The data that support the findings of this study are available within the article.

REFERENCES

- D. L. Partin, J. Heremans, D. T. Morelli, C. M. Thrush, C. H. Olk, and T. A. Perry, "Growth and characterization of epitaxial bismuth films," *Phys. Rev. B* **38**, 3818–3824 (1988).
- A. van Hulst, H. M. Jaeger, and S. Radelaar, "Epitaxial growth of bismuth films and bismuth-antimony heterostructures," *Phys. Rev. B* **52**, 5953–5961 (1995).
- S. Yaginuma, T. Nagao, J. T. Sadowski, M. Saito, K. Nagaoka, Y. Fujikawa, T. Sakurai, and T. Nakayama, "Origin of flat morphology and high crystallinity of ultrathin bismuth films," *Surf. Sci.* **601**, 3593–3600 (2007).
- J. C. Patrin, Y. Z. Li, M. Chander, and J. H. Weaver, "Sb and Bi on GaAs (110): Substrate-stabilized overlayer structures studied with scanning tunneling microscopy," *Phys. Rev. B* **46**, 10221–10231 (1992).
- T. Nagao, J. Sadowski, M. Saito, S. Yaginuma, Y. Fujikawa, T. Kogure, T. Ohno, Y. Hasegawa, S. Hasegawa, and T. Sakurai, "Nanofilm allotrope and phase transformation of ultrathin Bi film on Si(111)-7 \times 7," *Phys. Rev. Lett.* **93**, 105501 (2004).
- S. A. Scott, M. V. Kral, and S. A. Brown, "A crystallographic orientation transition and early stage growth characteristics of thin Bi films on HOPG," *Surf. Sci.* **587**, 175–184 (2005).
- J. Veletas, T. Hepp, K. Volz, and S. Chatterjee, "Bismuth surface segregation and disorder analysis of quaternary (Ga,In)(As,Bi)/InP alloys," *J. Appl. Phys.* **126**, 135705 (2019).
- A. Kawano, I. Konomi, H. Azuma, T. Hioki, and S. Noda, "Influence of bismuth as a surfactant on the growth of germanium on silicon," *J. Appl. Phys.* **74**, 4265–4267 (1993).
- Y. Fuseya, M. Ogata, and H. Fukuyama, "Transport properties and diamagnetism of Dirac electrons in bismuth," *J. Phys. Soc. Jpn.* **84**, 012001 (2015).
- P. J. Kowalczyk, O. Mahapatra, S. A. Brown, G. Bian, X. Wang, and T.-C. Chiang, "Electronic size effects in three-dimensional nanostructures," *Nano Lett.* **13**, 43–47 (2013).
- D. N. McCarthy, D. Robertson, P. J. Kowalczyk, and S. A. Brown, "The effects of annealing and growth temperature on the morphologies of Bi nanostructures on HOPG," *Surf. Sci.* **604**, 1273–1282 (2010).
- T. Hirahara, T. Nagao, I. Matsuda, G. Bihlmayer, E. V. Chulkov, Yu. M. Koroteev, and S. Hasegawa, "Quantum well states in ultrathin Bi films: Angle-resolved photoemission spectroscopy and first-principles calculations study," *Phys. Rev. B* **75**, 035422 (2007).
- C. A. Hoffman, J. R. Meyer, F. J. Bartoli, A. Di Venere, X. J. Yi, C. L. Hou, H. C. Wang, J. B. Ketterson, and G. K. Wong, "Semimetal-to-semiconductor transition in bismuth thin films," *Phys. Rev. B* **48**, 11431–11434 (1993).
- J. P. Heremans, C. M. Thrush, D. T. Morelli, and M.-C. Wu, "Thermoelectric power of bismuth nanocomposites," *Phys. Rev. Lett.* **88**, 216801 (2002).
- Y.-M. Lin, X. Sun, and M. S. Dresselhaus, "Theoretical investigation of thermoelectric transport properties of cylindrical Bi nanowires," *Phys. Rev. B* **62**, 4610–4623 (2000).
- P. M. Vereecken, L. Sun, P. C. Searson, M. Tanase, D. H. Reich, and C. L. Chien, "Magnetotransport properties of bismuth films on p-GaAs," *J. Appl. Phys.* **88**, 6529–6535 (2000).
- F. Y. Yang, K. Liu, K. Hong, D. H. Reich, P. C. Searson, and C. L. Chien, "Large magnetoresistance of electrodeposited single-crystal bismuth thin films," *Science* **284**, 1335–1337 (1999).
- Yu. M. Koroteev, G. Bihlmayer, J. E. Gayone, E. V. Chulkov, S. Blügel, P. M. Echenique, and Ph. Hofmann, "Strong spin-orbit splitting on Bi surfaces," *Phys. Rev. Lett.* **93**, 046403 (2004).
- G. Bihlmayer, O. Rader, and R. Winkler, "Focus on the Rashba effect," *New J. Phys.* **17**, 050202 (2015).
- F. Meier, H. Dil, J. Lobo-Checa, L. Patthey, and J. Osterwalder, "Quantitative vectorial spin analysis in angle-resolved photoemission: Bi/Ag(111) and Pb/Ag(111)," *Phys. Rev. B* **77**, 165431 (2008).
- K. Sakamoto, H. Kakuta, K. Sugawara, K. Miyamoto, A. Kimura, T. Kuzumaki, N. Ueno, E. Anese, J. Fujii, A. Kodama, T. Shishidou, H. Namatame, M. Taniguchi, T. Sato, T. Takahashi, and T. Oguchi, "Peculiar Rashba splitting originating from the two-dimensional symmetry of the surface," *Phys. Rev. Lett.* **103**, 156801 (2009).
- S. Agergaard, Ch. Søndergaard, H. Li, M. B. Nielsen, S. V. Hoffmann, Z. Li, and Ph. Hofmann, "The effect of reduced dimensionality on a semimetal: The electronic structure of the Bi(110) surface," *New J. Phys.* **3**, 15 (2001).
- C. R. Ast and H. Höchst, "Fermi surface of Bi(111) measured by photoemission spectroscopy," *Phys. Rev. Lett.* **87**, 177602 (2001).
- T. Guillet, C. Zucchetti, A. Marchionni, A. Hallal, P. Biagioni, C. Vergnaud, A. Marty, H. Okuno, A. Masseboeuf, M. Finazzi, F. Ciccacci, M. Chshiev, F. Bottegoni, and M. Jamet, "Spin orbitronics at a topological insulator-semiconductor interface," *Phys. Rev. B* **101**, 184406 (2020).
- Z.-H. Pan, E. Vescovo, A. V. Fedorov, D. Gardner, Y. S. Lee, S. Chu, G. D. Gu, and T. Valla, "Electronic structure of the topological insulator Bi₂Se₃ using angle-resolved photoemission spectroscopy: Evidence for a nearly full surface spin polarization," *Phys. Rev. Lett.* **106**, 257004 (2011).
- A. Manchon, H. C. Koo, J. Nitta, S. M. Frolov, and R. A. Duine, "New perspectives for Rashba spin-orbit coupling," *Nat. Mater.* **14**, 871–882 (2015).
- P. D. Johnson and S. L. Hulbert, "Inverse photoemission," *Rev. Sci. Instrum.* **61**, 2277–2288 (1990).
- R. M. Feenstra, V. Ramachandran, and H. Chen, "Recent developments in scanning tunneling spectroscopy of semiconductor surfaces," *Appl. Phys. A: Mater. Sci. Process.* **72**, S193–9 (2001).
- R. M. Feenstra, "Electronic states of metal atoms on the GaAs(110) surface studied by scanning tunneling microscopy," *Phys. Rev. Lett.* **63**, 1412–1415 (1989).
- A. B. McLean and F. J. Himpsel, "Resonant inverse-photoemission study of layer-dependent surface states at the epitaxial GaAs(110)-Bi interface," *Phys. Rev. B* **40**, 8425–8430 (1989).
- S. D. Stolwijk, A. B. Schmidt, M. Donath, K. Sakamoto, and P. Krüger, "Rotating spin and giant splitting: Unoccupied surface electronic structure of Tl/Si(111)," *Phys. Rev. Lett.* **111**, 176402 (2013).
- S. N. P. Wissing, C. Eibl, A. Zumbülte, A. B. Schmidt, J. Braun, J. Minár, H. Ebert, and M. Donath, "Rashba-type spin splitting at Au(111) beyond the Fermi level: The other part of the story," *New J. Phys.* **15**, 105001 (2013).
- J. Gou, L.-J. Kong, W.-B. Li, S.-X. Sheng, H. Li, S. Meng, P. Cheng, K.-H. Wu, and L. Chen, "Scanning tunneling microscopy investigations of unoccupied surface states in two-dimensional semiconducting β - $\sqrt{3} \times \sqrt{3}$ -Bi/Si(111) surface," *Phys. Chem. Chem. Phys.* **20**, 20188–20193 (2018).
- S. Hatta, T. Aruga, Y. Ohtsubo, and H. Okuyama, "Large Rashba spin splitting of surface resonance bands on semiconductor surface," *Phys. Rev. B* **80**, 113309 (2009).
- F. Bottegoni, A. Calloni, G. Bussetti, A. Camera, C. Zucchetti, M. Finazzi, L. Duò, and F. Ciccacci, "Spin polarized surface resonance bands in single layer Bi on Ge(111)," *J. Phys.: Condens. Matter* **28**, 195001 (2016).
- S. Hatta, Y. Ohtsubo, S. Miyamoto, H. Okuyama, and T. Aruga, "Epitaxial growth of Bi thin films on Ge(111)," *Appl. Surf. Sci.* **256**, 1252–1256 (2009).
- C. Zucchetti, M.-T. Dau, F. Bottegoni, C. Vergnaud, T. Guillet, A. Marty, C. Beigné, S. Gambarelli, A. Picone, A. Calloni, G. Bussetti, A. Brambilla, L. Duò, F. Ciccacci, P. K. Das, J. Fujii, I. Vobornik, M. Finazzi, and M. Jamet, "Tuning spin-charge interconversion with quantum confinement in ultrathin bismuth films," *Phys. Rev. B* **98**, 184418 (2018).

- ³⁸R. D. Bringans and H. Höchst, "Electronic structure of Ge(111) and Ge(111): H from angle-resolved-photoemission measurements," *Phys. Rev. B* **25**, 1081–1089 (1982).
- ³⁹C. Zucchetti, F. Bottegoni, A. Calloni, G. Bussetti, L. Duò, M. Finazzi, and F. Ciccacci, "Evolution of the structural and electronic properties of thin Bi films on Ge(111)," *J. Phys. Conf. Ser.* **903**, 012024 (2017).
- ⁴⁰G. Berti, A. Calloni, A. Brambilla, G. Bussetti, L. Duò, and F. Ciccacci, "Direct observation of spin-resolved full and empty electron states in ferromagnetic surfaces," *Rev. Sci. Instrum.* **85**, 073901 (2014).
- ⁴¹D. T. Pierce, R. J. Celotta, G.-C. Wang, W. N. Unertl, A. Galejs, C. E. Kuyatt, and S. R. Mielczarek, "The GaAs spin polarized electron source," *Rev. Sci. Instrum.* **51**, 478–499 (1980).
- ⁴²Y. Ohtsubo, H. Muto, K. Yaji, S. Hatta, H. Okuyama, and T. Aruga, "Structure determination of Pb/Ge(111)- β - $(\sqrt{3} \times \sqrt{3})R30^\circ$ by dynamical low-energy electron diffraction analysis and first-principles calculation," *J. Phys. Condens. Matter* **23**, 435001 (2011).
- ⁴³D. Lükermann, S. Banyoudeh, C. Brand, S. Sologub, H. Pfnür, and C. Tegenkamp, "Growth of epitaxial Bi-films on vicinal Si(111)," *Surf. Sci.* **621**, 82–87 (2014).
- ⁴⁴K. Nagase, I. Kokubo, S. Yamazaki, K. Nakatsuji, and H. Hirayama, "Structure and growth of Bi(110) islands on Si(111) 3×3 -B substrates," *Phys. Rev. B* **97**, 195418 (2018).
- ⁴⁵L. Gavioli, M. G. Betti, P. Casarini, and C. Mariani, "Overlay growth and electronic properties of the Bi/GaSb(110) interface," *Phys. Rev. B* **51**, 16822–16831 (1995).
- ⁴⁶A. Kakizaki, M. Niwano, H. Yamakawa, K. Soda, S. Suzuki, H. Sugawara, H. Kato, T. Miyahara, and T. Ishii, "A UPS study of liquid and solid bismuth using synchrotron radiation," *J. Phys. F Met. Phys.* **18**, 2617–2624 (1988).
- ⁴⁷G. Bian, T. Miller, and T.-C. Chiang, "Electronic structure and surface-mediated metastability of Bi films on Si(111)- 7×7 studied by angle-resolved photoemission spectroscopy," *Phys. Rev. B* **80**, 245407 (2009).
- ⁴⁸Y. Hu, T. J. Wagener, M. B. Jost, and J. H. Weaver, "Evolution of empty-state bands for Bi/GaAs(110): From Bi zigzag chains to ordered overlayers," *Phys. Rev. B* **40**, 1146–1151 (1989).
- ⁴⁹G. Bian, X. Wang, T. Miller, T.-C. Chiang, P. J. Kowalczyk, O. Mahapatra, and S. A. Brown, "First-principles and spectroscopic studies of Bi(110) films: Thickness-dependent Dirac modes and property oscillations," *Phys. Rev. B* **90**, 195409 (2014).
- ⁵⁰F. Donati, P. Sessi, S. Achilli, A. Li Bassi, M. Passoni, C. S. Casari, C. E. Bottani, A. Brambilla, A. Picone, M. Finazzi, L. Duò, M. I. Trioni, and F. Ciccacci, "Scanning tunneling spectroscopy of the Fe(001)- $p(1 \times 1)$ O surface," *Phys. Rev. B* **79**, 195430 (2009).
- ⁵¹J. I. Pascual, G. Bihlmayer, Yu. M. Koroteev, H.-P. Rust, G. Ceballos, M. Hansmann, K. Horn, E. V. Chulkov, S. Blügel, P. M. Echenique, and Ph. Hofmann, "Role of spin in quasiparticle interference," *Phys. Rev. Lett.* **93**, 196802 (2004).
- ⁵²G. van der Laan, "Zen and the art of dichroic photoemission," *J. Electron Spectrosc. Relat. Phenom.* **200**, 143–159 (2015).
- ⁵³J. Henk, T. Scheunemann, S. V. Halilov, and R. Feder, "Magnetic dichroism and electron spin polarization in photoemission: Analytical results," *J. Phys.: Condens. Matter* **8**, 47–65 (1996).
- ⁵⁴E. Tamura, W. Piepke, and R. Feder, "New spin-polarization effect in photoemission from nonmagnetic surfaces," *Phys. Rev. Lett.* **59**, 934–937 (1987).
- ⁵⁵H. Wortelen, H. Mirhosseini, K. Miyamoto, A. B. Schmidt, J. Henk, and M. Donath, "Tuning the spin signal from a highly symmetric unpolarized electronic state," *Phys. Rev. B* **91**, 115420 (2015).
- ⁵⁶H. Bentmann, H. Maaß, E. E. Krasovskii, T. R. F. Peixoto, C. Seibel, M. Leandersson, T. Balasubramanian, and F. Reinert, "Strong linear dichroism in spin-polarized photoemission from spin-orbit-coupled surface states," *Phys. Rev. Lett.* **119**, 106401 (2017).
- ⁵⁷R. Noguchi, K. Kuroda, K. Yaji, K. Kobayashi, M. Sakano, A. Harasawa, T. Kondo, F. Komori, and S. Shin, "Direct mapping of spin and orbital entangled wave functions under interband spin-orbit coupling of giant Rashba spin-split surface states," *Phys. Rev. B* **95**, 041111 (2017).
- ⁵⁸S. N. P. Wissing, A. B. Schmidt, H. Mirhosseini, J. Henk, C. R. Ast, and M. Donath, "Ambiguity of experimental spin information from states with mixed orbital symmetries," *Phys. Rev. Lett.* **113**, 116402 (2014).